Expanded View Figures

Figure EV1. Elevated localization of MIRO-1 in the fragmented mitochondria.

A Representative confocal images show mito::GFP signal for mitochondrial morphology in WT, *fzo-1(tm1133)*, and *eat-3(tm1107)* mutants. Fragmented mitochondria are observed in both *fzo-1(tm1133)* and *eat-3(tm1107)* mutants.

B Schematic of the TMRE staining method in *Caenorhabditis elegans* epidermis. TMRE is added to the NGM plate for 2 h, and then L4 stage worms are transferred to the plate to culture 12 h before being subjected to confocal imaging.

C Representative confocal microscopy images show TMRE signal in WT and *fzo-1(tm1133)* mutants. Red fluorescence shows TMRE staining, and green fluorescence shows mitochondria tagged with GFP.

D Quantitation of TMRE fluorescence normalized to mito::GFP in *fzo-1(tm1133)* mutants compared with WT, $n > 300$ mitochondria.

E The correlation between the mitochondrial size and MIRO-1 content. Spearman's correlation analysis of the mitochondrial size and MIRO-1 expression in *fzo-1* mutant. $n = 196$ mitochondria.

F The correlation between mitochondrial size and mitochondrial membrane potential. Spearman's correlation analysis of the mitochondrial size and TMRE intensity in *fzo-1* mutants. $n = 187$ mitochondria.

G Real-time PCR test for *miro-1* expression in WT and *fzo-1(tm1133)* mutants. $n = 3$, biological replicates.

H Representative confocal images show the GFP::MIRO-1 and TMRE staining in WT and *eat-3(tm1107)* mutants.

I Plot analysis of GFP::MIRO-1 and TMRE signals.

Data information: Data are shown as the mean ± SEM. ***$P < 0.001$ (unpaired *t*-test). Scale bars, 10 and 5 μm (zoom in).

© 2023 The Authors

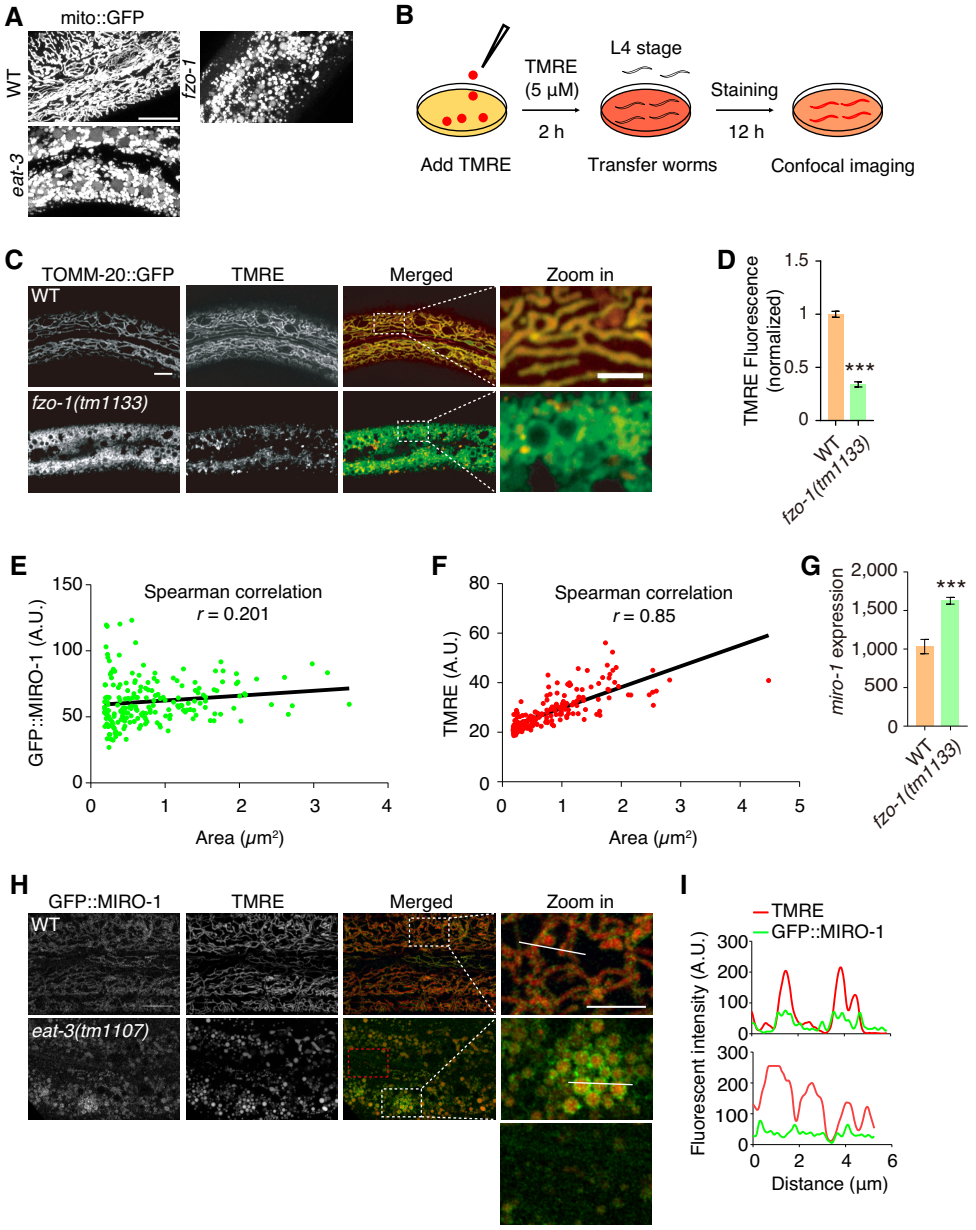

Figure EV1.

© 2023 The Authors

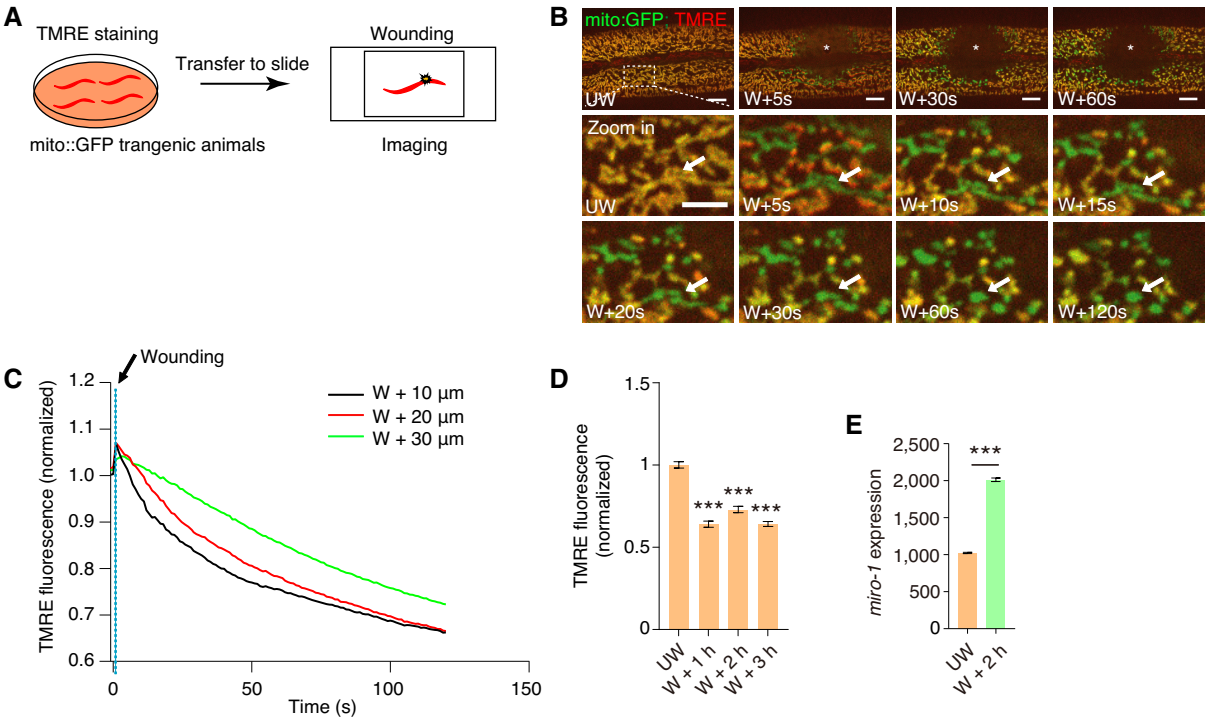

Figure EV2. Wounding induces immediate reduction of ΔΨm.

A Schematic representation of the ΔΨm determination upon laser wounding in *Caenorhabditis elegans* epidermis.

B Representative confocal images show TMRE signal after laser wounding. The bottom panels show the changes in mitochondrial morphology and ΔΨm in magnification images. The white arrow indicates a tubular mitochondrion depolarizing quickly, followed by fragmentation.

C Quantitation of the ratio of TMRE fluorescence normalized to mito::GFP at the wound site in (B). The reduction of TMRE is first at the wound site and then spreads to the neighboring region.

D Quantitation of TMRE fluorescence to mito::GFP at different time points after wounding. $n > 300$ mitochondria.

E Quantitative PCR is used to measure *miro-1* expression before and 2 h after wounding treatment.

Data information: Data are shown as the mean ± SEM. ***$P < 0.001$ (unpaired *t*-test or one-way ANOVA test). Scale bars, 10 and 5 μm (zoom in).

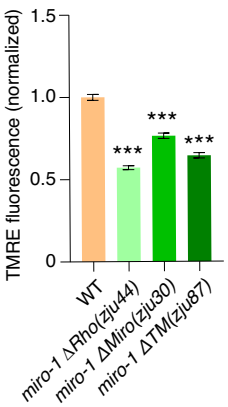

Figure EV3. MIRO-1 is required for the maintenance of ΔΨm.

Quantification of the ratio of TMRE fluorescence normalized mito::GFP in WT, *miro-1ΔRho*, miro-1*ΔMiro*, and miro-1*ΔTM* (transmembrane domain) deletion mutants. n > 300 mitochondria. Data are shown as the mean ± SEM. ***P < 0.001 (one-way ANOVA test).

© 2023 The Authors

Figure EV4. Identification of MIRO-1 interaction proteins via PUP-IT system in vivo.

A Schematic representation of the PUP-IT system. PafA (yellow) is fused to MIRO-1 (orange) and mediates Bio-Pup (E) (blue) modification of prey protein (green). The modified prey proteins are pulldown by streptavidin-coated beads and detected by silver staining and mass spectrometry.

B Silver staining (left panel) shows the proteins pulldown by streptavidin-coated beads in PafA-MIRO-1, Bio-Pup (E), and PUP-IT groups. Immunoblot (middle and right corrective) shows many streptavidin-bonded and biotin-labeled proteins by anti-streptavidin and anti-biotin antibodies.

C Table summarizing the names, mitochondrial localizations, and biological functions of 10 of 13 mitochondrial proteins identified in (Fig 4C).

D Representative confocal images show the colocalization between P*col-19*::VDAC-1::GFP and mKate2::MIRO-1.

E Plot analysis shows partial colocalization between P*col-19*::VDAC-1::GFP and mKate2::MIRO-1 in (D).

F Immunoblot analysis showing the immunoprecipitation of GFP::MIRO-1 (ΔTM) and GFP::MIRO-1 (TM), respectively, by GFP nanobody-conjugated beads. GFP::MIRO-1 (TM) is weakly interacting with VDAC-1. However, GFP::MIRO-1 (ΔTM) is strongly interacting with VDAC-1.

G Immunoblot shows the immunoprecipitation of GFP::MIRO-1 (nGTPase) and GFP::MIRO-1 C-part (EF-hands + cGTPase), respectively, by GFP nanobody-conjugated beads. GFP::MIRO-1 C-part is strongly interacting with VDAC-1 (* indicating nonspecific band).

Data information: Scale bars, 10 and 5 μm (zoom in).

© 2023 The Authors

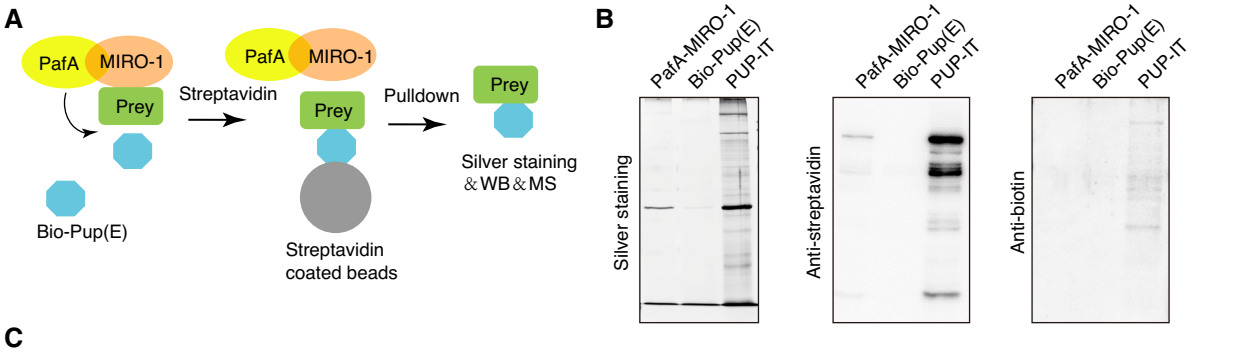

C

Protein	Location	Function
VDAC-1	MOM	Porin activity and voltage-gated anion channel activit
ASG-2	MIM	Proton transmembrane transporter activity
SUCA-1	MIM	ATP binding activity; magnesium ion binding activity; and succinate-CoA ligase (ADP-forming) activity
F58F12.1	MIM	Proton-transporting ATP synthase activity, rotational mechanism
SDHB-1	MIM	Iron-sulfur cluster binding activity and ubiquinone binding activity
PHDA-1	Matrix	Pyruvate dehydrogenase (acetyl-transferring) activity
OATR-1	Matrix	Ornithine (lysine) transaminase activity; ornithine-oxo-acid transaminase activity; and pyridoxal phosphate binding activity
DBT-1	Matrix	Acetyltransferase activity; Dihydrolipoyllysine-residue (2-methylpropanoyl) transferase activity
DLAT-1	Matrix	Dihydrolipoyllysine-residue acetyltransferase activity
MMCM-1	Matrix	Cobalamin binding activity; metal ion binding activity; and methylmalonyl-CoA mutase activity

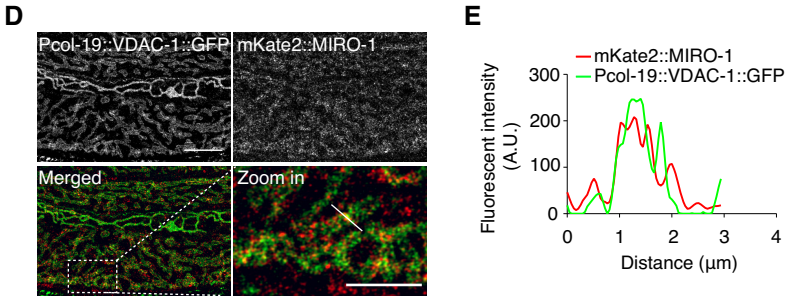

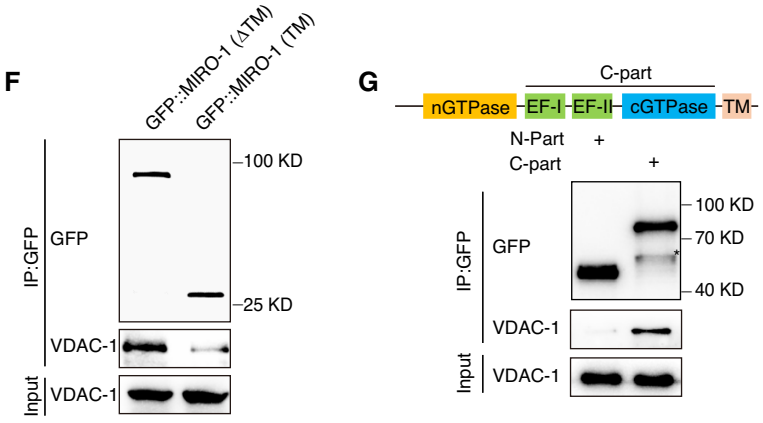

Figure EV4.

© 2023 The Authors

Figure EV5. The regulation of mitochondrial functions and GTPase activity by the interaction of MIRO-1 and VDAC-1.

A Immunoprecipitation of GFP::MIRO-1 C-part and GFP::MIRO-1 C-part(E473G), respectively, by GFP nanobody-conjugated beads.
B Immunoprecipitation of VDAC-1::GFP and VDAC-1(K163G)::GFP with mKate2::MIRO-1 using GFP nanobody-conjugated beads.
C Immunoblot analysis of purified MIRO-1::His, MIRO-1 (E473G)::His, and VDAC-1::His proteins after BMH crosslinking by His antibody. The black arrow indicates the potential bands of the MIRO-1–VDAC-1 interaction complex.
D-F Coomassie brilliant blue staining of MIRO-1 and VDAC-1 proteins after BMH crosslinking. The high molecular weight is indicated by a red box and cut for protein identification by MS in (E and F). Fifty unique peptides of MIRO-1 and 14 unique peptides of VDAC-1 were identified.
G Quantification of $\Delta\Psi$m in crude isolated mitochondria from WT and *miro-1(E473G)* mutants (ratio of JC-1 stain red fluorescence to green fluorescence). $n = 3$, biological replicates.
H ATP content in crude isolated mitochondria of WT animals and *miro-1(E473G)* mutants. Quantification is conducted with a commercial luminescence kit. $n = 3$, biological replicates.
I MIRO-1 GTPase activity analysis after GFP beads pulldown in *GFP::MIRO-1* and *GFP::MIRO-1(E473G)* worms were measured by GTPase assay kit. GFP expressions were measured as a normalized control. $n = 3$, biological replicates.
J GTPase activity analysis of purified MIRO-1::His and MIRO-1(E473G)::His were measured by GTPase assay kit. Protein concentrations were measured as a normalized control. $n = 3$, technical replicates.

Data information: Data are shown as the mean ± SEM. $^{**}P < 0.01$, $^{***}P < 0.001$ (unpaired *t*-test).

© 2023 The Authors

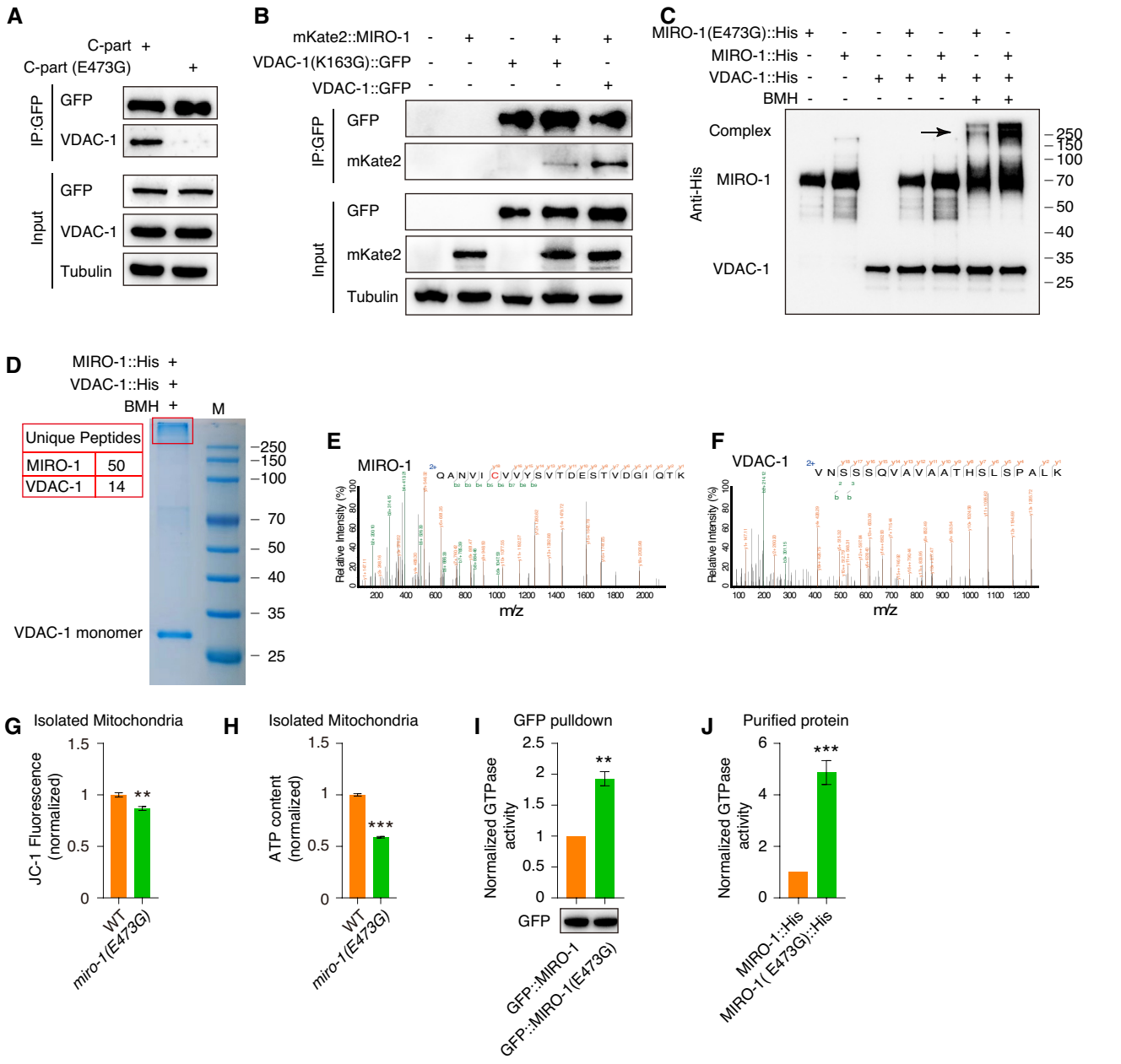
A
C-part +
C-part (E473G) +
IP:GFP
GFP
VDAC-1
Input
GFP
VDAC-1
Tubulin
B
mKate2::MIRO-1 - + - + +
VDAC-1(K163G)::GFP - - + + -
VDAC-1::GFP - - - - +
IP:GFP
GFP
mKate2
Input
GFP
mKate2
Tubulin
C
MIRO-1(E473G)::His + - - + - + -
MIRO-1::His - + - - + - +
VDAC-1::His - - + + + + +
BMH - - - - - + +
Anti-His
Complex
MIRO-1
VDAC-1
250
150
100
70
50
40
35
25
D
MIRO-1::His +
VDAC-1::His +
BMH +
M
Unique Peptides
MIRO-1 50
VDAC-1 14
VDAC-1 monomer
250
150
100
70
50
40
35
25
E
MIRO-1
Q A N V I C V V Y S V T D E S T V D G I Q T K
Relative Intensity (%)
m/z
F
VDAC-1
V N S S S Q V A V A A T H S L S P A L K
Relative Intensity (%)
m/z
G
Isolated Mitochondria
JC-1 Fluorescence (normalized)
WT
miro-1(E473G)
H
Isolated Mitochondria
ATP content (normalized)
WT
miro-1(E473G)
I
GFP pulldown
Normalized GTPase activity
GFP
GFP::MIRO-1
GFP::MIRO-1(E473G)
J
Purified protein
Normalized GTPase activity
MIRO-1::His
MIRO-1(E473G)::His

Figure EV5.